

# Dimolybdenum Bis((*S,S,S*)-triisopropanolamate(3<sup>-</sup>)): A Blue Compound with an Unusual Mo–Mo Triple Bond<sup>‡</sup>

Malcolm H. Chisholm,<sup>\*,1a</sup> Ann M. Macintosh,<sup>1a</sup> John C. Huffman,<sup>1a</sup> Dedong Wu,<sup>1a</sup>  
Ernest R. Davidson,<sup>\*,1a</sup> Robin J. H. Clark,<sup>\*,1b</sup> and Steven Firth<sup>1b</sup>

Department of Chemistry, Indiana University, Bloomington, Indiana 47405, and Christopher Ingold Laboratories, University College London, London WC1H 0AJ, United Kingdom

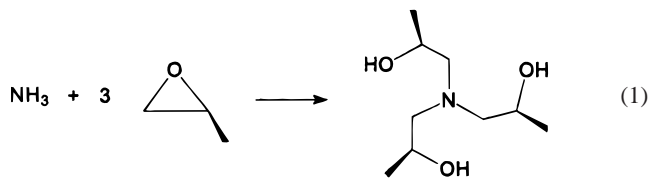
Received November 22, 1999

Mo<sub>2</sub>(O<sup>t</sup>Bu)<sub>6</sub> and Mo<sub>2</sub>(NMe<sub>2</sub>)<sub>6</sub> each react with (*S,S,S*)-triisopropanolamine (2 equiv) in benzene to yield dimolybdenum bis((*S,S,S*)-isopropanolamate(3<sup>-</sup>)), Mo<sub>2</sub>[(OC-(*S*)-HMeCH<sub>2</sub>)<sub>3</sub>N]<sub>2</sub> (M≡M), as a blue crystalline solid. Cell parameters at -160 °C: *a* = 17.389(6) Å, *b* = 10.843(3) Å, *c* = 10.463(3) Å, β = 125.28(1)°, *Z* = 2 in space group C2. The molecular structure involves an Mo<sub>2</sub> unit inside an O<sub>6</sub>N<sub>2</sub> distorted cubic box. The Mo<sub>2</sub> axis is disordered about three positions with occupancy factors of ca. 45%, 45%, and 10%. Despite this disorder, the molecular structure is shown to contain a central Mo≡Mo unit of distance 2.15(3) Å coordinated to two triolate ligands which each have two chelating arms and one that spans the Mo≡Mo bond. The local Mo<sub>2</sub>O<sub>6</sub>N<sub>2</sub> moiety has approximate C<sub>2h</sub> symmetry, and the Mo–N distances are long, 2.4 Å. The <sup>1</sup>H and <sup>13</sup>C{<sup>1</sup>H} NMR spectra recorded in benzene-*d*<sub>6</sub> are consistent with the geometry found in the solid-state structure. The blue color arises from weak absorptions, ε ~ 150 dm<sup>3</sup> mol<sup>-1</sup> cm<sup>-1</sup>, at 580 and 450 nm in the visible region of the electronic absorption spectrum. Raman spectra recorded in KCl reveal pronounced resonance effects with excitation wavelengths of 488.0, 514.5, and 568.2 nm, particularly for the 322 cm<sup>-1</sup> band, which can probably be assigned to ν(Mo≡Mo). The electronic structure of this compound is investigated by B3LYP DFT calculations, and a comparison is made with the more typical ethane-like (*D*<sub>3d</sub>) Mo<sub>2</sub>(OR)<sub>6</sub> compounds is presented. The distortion imposed on the molecule by the triisopropanolamate(3<sup>-</sup>) ligands removes the degeneracy of the M–M π molecular orbitals. The HOMO and SHOMO are both M–M π and M–O σ\* in character, while the LUMO is M–M π\* and the SLUMO is predominantly M–O σ\* with metal sp character. The calculated singlet–singlet transition energies are compared with those implicit in the observed electronic spectrum.

## Introduction

The development of the chemistry of triple-bonded complexes of molybdenum and tungsten has principally involved the use of sterically demanding monodentate ligands such as alkyl, alkoxide, amide, thiolate, etc., as in the homoleptic series M<sub>2</sub>X<sub>6</sub> or in the mixed-ligated species M<sub>2</sub>X<sub>6-n</sub>Y<sub>n</sub>, in which *n* = 1–3 and one of the groups X and Y is less sterically demanding than the other, as in the M<sub>2</sub>Cl<sub>2</sub>(NMe<sub>2</sub>)<sub>4</sub> compounds.<sup>2,3</sup> Certain bidentate ligands such as carboxylates, carbamates, and dithiophosphates have also been employed, and the central M≡M moiety is preserved in compounds such as W<sub>2</sub>Me<sub>2</sub>(O<sub>2</sub>CNEt<sub>2</sub>)<sub>4</sub> and W<sub>2</sub>(O<sub>2</sub>CNMe<sub>2</sub>)<sub>6</sub>.<sup>2,3</sup> Recently, we have been investigating the chemistry of the M<sub>2</sub><sup>6+</sup> unit with sterically encumbered diolates and biphenoxides.<sup>4–6</sup> The use of these ligands has allowed us to interrogate the mechanisms of substitution about

the M<sub>2</sub><sup>6+</sup> center because the kinetic and thermodynamic products do not interconvert readily. Similarly, with the use of the *p*-*tert*-butylcalix(4)arene derivatives, we have seen interesting substitution patterns and accessed both dumbbell and bridging (*μ*-η<sup>2</sup>,η<sup>2</sup>) forms of coordination.<sup>7</sup> We were attracted to the use of chiral trialkanolamines, such as (*S,S,S*)-triisopropanolamine, which is readily accessible from the reaction shown in eq 1.



Nugent and Harlow reported the use of these chiral trialkanolamines in the synthesis of early transition metal alkoxides of the type LTi(O<sup>t</sup>Pr)<sub>3</sub>, LV=O, and LM(OEt)<sub>2</sub> (M = Nb, Ta) where L = the trialkanolamate(3<sup>-</sup>).<sup>8</sup> We describe here the synthesis of the Mo<sub>2</sub>L<sub>2</sub> compound, where L = (*S,S,S*)-triisopropanolamate(3<sup>-</sup>), which, as a result of the steric constraints of the ligand and the propensity of the metal atoms to maintain an unbridged Mo≡Mo bond, has an unusual structure wherein the degeneracy of the typical cylindrical triple bonds seen for M<sub>2</sub>X<sub>6</sub> compounds is removed.

<sup>‡</sup> This paper is dedicated to Professor F. A. Cotton on the occasion of his 70th birthday.

- (1) (a) Indiana University. E-mail: chisholm@chemistry.ohio-state.edu; davidson@indiana.edu. (b) University College London. E-mail: r.j.h.clark@ucl.ac.uk.
- (2) Cotton, F. A.; Walton, R. A. *Multiple Bonds Between Metal Atoms*, 2nd ed.; Oxford University Press: Oxford, U.K., 1993.
- (3) Chisholm, M. H. *Acc. Chem. Res.* **1990**, *23*, 419.
- (4) Chisholm, M. H.; Parkin, I. P.; Foltling, K.; Lobkovsky, E. *Inorg. Chem.* **1997**, *36*, 1636.
- (5) Chisholm, M. H.; Huang, J.-H.; Huffman, J. C.; Parkin, I. P. *Inorg. Chem.* **1997**, *36*, 1642.
- (6) Chisholm, M. H.; Foltling, K.; Streib, W. E.; Wu, D. *Inorg. Chem.* **1998**, *37*, 50.

(7) Chisholm, M. H.; Foltling, K.; Streib, W. E.; Wu, D. *Chem. Commun.* **1998**, 379; *Inorg. Chem.* **1999**, *38*, 5219.

(8) Nugent, W. A.; Harlow, R. L. *J. Am. Chem. Soc.* **1994**, *116*, 6142.

## Results and Discussion

**Synthesis.** The reactions of  $\text{Mo}_2(\text{O}^t\text{Bu})_6^9$  and  $\text{Mo}_2(\text{NMe}_2)_6^{10}$  with (S,S,S)-triisopropanolamine,  $\text{LH}_3$  (2 equiv), in benzene lead to the formation of  $\text{Mo}_2\text{L}_2$  in essentially quantitative yield. Crystallization from benzene yields blue crystals of  $\text{Mo}_2\text{L}_2$  which are air stable for short periods of time ( $\sim 1$  day). Related reactions involving  $\text{W}_2(\text{O}^t\text{Bu})_6^{11}$  and  $\text{W}_2(\text{NMe}_2)_6^{12}$  yield a green compound which is thermally unstable and has not been properly characterized beyond obtaining an  $^1\text{H}$  NMR spectrum from a freshly prepared sample. By analogy with the  $^1\text{H}$  NMR spectrum of  $\text{Mo}_2\text{L}_2$  (vide infra), we can postulate that the structure of  $\text{W}_2\text{L}_2$  is analogous to that of  $\text{Mo}_2\text{L}_2$ . Why the ditungsten complex is thermally unstable is not clear.

Reactions of  $\text{M}_2(\text{O}^t\text{Bu})_6$  and  $\text{M}_2(\text{NMe}_2)_6$ , where  $\text{M} = \text{Mo}$  or  $\text{W}$ , with triethanolamine in benzene yield brown precipitates which are insoluble in hydrocarbon solvents and other common organic solvents. We believe that these products are oligomers and propose that the presence of the methyl group (or possibly other alkyl groups) is necessary for steric protection of the central  $\text{M}_2^{6+}$  unit.

**NMR Spectra.** The  $^1\text{H}$  NMR spectra of  $\text{Mo}_2\text{L}_2$  in toluene- $d_8$  are essentially temperature independent. There are three methyl doublets at high field, ca. 1.2 ppm, and three methine resonances, two at low field, 5.5 and 5.3 ppm, and one at notably higher field, 3.4 ppm. Clearly, there are three different orientations of the  $\text{OCHMeCH}_2$  groups with respect to the  $\text{Mo}\equiv\text{Mo}$  bond and the magnetic anisotropy of the latter is responsible for the shielding and deshielding effects on the methine protons. A COSY spectrum was obtained which allowed the connectivity of the resonances to be established for each  $\text{OCHMeCH}_2$  group. Data are given in the Experimental Section.

**Solid-State Crystal and Molecular Structures.** The blue crystals of  $\text{Mo}_2\text{L}_2$  proved to be troublesome with respect to obtaining a satisfactory molecular structure by single-crystal X-ray crystallography. Crystals were obtained from a variety of solvents (benzene, toluene, and THF), but in all cases, the solutions of the structures had a common problem. The structural work reported here was performed on a crystal grown in benzene which had the solvate formula  $\text{Mo}_2\text{L}_2 \cdot 2\text{C}_6\text{H}_6$ .

In the space group  $C_2$ , there are two equivalent molecules in the unit cell. The problem with the solution is a common one for molecules of the type wherein an  $\text{M}_2^{n+}$  unit is inside a box, namely, that while the ligand atom positions are relatively well defined (fixed), the  $\text{Mo}-\text{Mo}$  axis is disordered over three possible positions.<sup>13</sup> In this case, the  $\text{O}_6\text{N}_2$  skeleton conforms to a distorted cube and the  $\text{Mo}_2^{6+}$  unit is disordered principally about two positions with equal occupancy, 45%, and to a lesser extent, 10%, about the third.

A ball-and-stick drawing of the molecular structure is shown in Figure 1. Each molecule has a crystallographically imposed  $C_2$  axis of symmetry, and the central  $\text{Mo}_2\text{N}_2\text{O}_6$  core has virtual  $C_{2h}$  symmetry. Listings of selected bond distances and bond angles for the three disordered molecules are given in Tables 1 and 2. With the disorder, the agreement of  $\text{M}-\text{M}$ ,  $\text{M}-\text{O}$ , and  $\text{M}-\text{N}$  distances is poor. However, there is no doubt about the

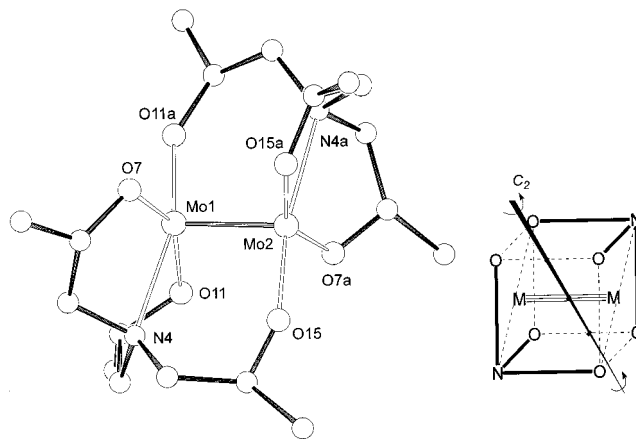


**Figure 1.** Ball-and-stick drawing of  $\text{Mo}_2\text{L}_2$  showing one of the principal orientations of the  $\text{Mo}-\text{Mo}$  unit.

**Table 1.** Selected Bond Distances ( $\text{\AA}$ ) of  $\text{Mo}_2\text{L}_2$

$\text{Mo}(1)-\text{Mo}(2)$	2.1770(11)	$\text{Mo}(2)-\text{O}(15a)$	1.944(7)
$\text{Mo}(1)-\text{O}(7)$	1.897(5)	$\text{Mo}(2)-\text{N}(4a)$	2.356(5)
$\text{Mo}(1)-\text{O}(11)$	1.859(9)	$\text{Mo}(3)-\text{Mo}(3)$	2.14(2)
$\text{Mo}(1)-\text{O}(11a)$	2.017(9)	$\text{Mo}(3)-\text{O}(7)$	2.06(1)
$\text{Mo}(1)-\text{N}(4)$	2.382(5)	$\text{Mo}(3)-\text{O}(11)$	1.76(2)
$\text{Mo}(2)-\text{O}(7)$	2.018(6)	$\text{Mo}(3)-\text{O}(15)$	2.07(2)
$\text{Mo}(2)-\text{O}(15)$	1.884(7)	$\text{Mo}(3)-\text{N}(4)$	2.44(1)

**Table 2.** Selected Bond Angles (deg) of  $\text{Mo}_2\text{L}_2$

$\text{Mo}(2)-\text{Mo}(1)-\text{O}(7)$	101.3(3)	$\text{O}(7a)-\text{Mo}(2)-\text{O}(15)$	98.6(3)
$\text{Mo}(2)-\text{Mo}(1)-\text{O}(11)$	103.7(3)	$\text{O}(7a)-\text{Mo}(2)-\text{N}(4a)$	72.1(2)
$\text{Mo}(2)-\text{Mo}(1)-\text{O}(11a)$	94.3(3)	$\text{O}(15a)-\text{Mo}(2)-\text{O}(15)$	98.7(7)
$\text{Mo}(2)-\text{Mo}(1)-\text{N}(4)$	97.8(3)	$\text{O}(15a)-\text{Mo}(2)-\text{N}(4)$	83.8(4)
$\text{O}(7)-\text{Mo}(1)-\text{O}(11)$	146.7(3)	$\text{O}(15)-\text{Mo}(2)-\text{N}(4)$	158.7(3)
$\text{O}(7)-\text{Mo}(1)-\text{O}(11a)$	99.5(3)	$\text{Mo}(3a)-\text{Mo}(3)-\text{O}(7a)$	94.1(6)
$\text{O}(7)-\text{Mo}(1)-\text{N}(4)$	73.4(2)	$\text{Mo}(3a)-\text{Mo}(3)-\text{O}(11)$	102.3(6)
$\text{O}(11)-\text{Mo}(1)-\text{O}(11a)$	100.1(7)	$\text{Mo}(3a)-\text{Mo}(3)-\text{O}(15)$	100.2(4)
$\text{O}(11)-\text{Mo}(1)-\text{N}(4)$	81.7(4)	$\text{Mo}(3a)-\text{Mo}(3)-\text{N}(4)$	96.4(6)
$\text{O}(11a)-\text{Mo}(1)-\text{N}(4)$	167.0(3)	$\text{O}(7a)-\text{Mo}(3)-\text{O}(11)$	102.7(9)
$\text{Mo}(1)-\text{Mo}(2)-\text{O}(7a)$	97.3(2)	$\text{O}(7a)-\text{Mo}(3)-\text{O}(15)$	93.3(8)
$\text{Mo}(1)-\text{Mo}(2)-\text{O}(15)$	99.1(3)	$\text{O}(7a)-\text{Mo}(3)-\text{N}(4)$	167.3(8)
$\text{Mo}(1)-\text{Mo}(2)-\text{O}(15a)$	102.1(3)	$\text{O}(11)-\text{Mo}(3)-\text{O}(15)$	151.2(6)
$\text{Mo}(1)-\text{Mo}(2)-\text{N}(4a)$	101.1(2)	$\text{O}(11)-\text{Mo}(3)-\text{N}(4)$	81.9(7)
$\text{O}(7a)-\text{Mo}(2)-\text{O}(15a)$	151.5(2)	$\text{O}(15)-\text{Mo}(3)-\text{N}(4)$	77.9(6)

basic coordination geometry of the  $\text{Mo}_2^{6+}$  unit being that shown in Figure 1. (The minor disordered molecule has the crystallographic  $C_2$  axis perpendicular to the  $\text{M}-\text{M}$  axis.) Of particular note is the fact that the  $\text{Mo}-\text{N}$  distances are very long, ca. 2.4  $\text{\AA}$ , indicative of very weak  $\text{N}$  to  $\text{Mo}$  bonding. The  $\text{M}-\text{M}$  distances are typical for an  $(\text{Mo}\equiv\text{Mo})^{6+}$  unit.<sup>2</sup> The local  $\text{MoO}_3$  coordination is that of a distorted T, and thus the  $\text{Mo}_2\text{O}_6$  skeleton may be related to that of the typical  $D_{3d}$ - $\text{Mo}_2(\text{OR})_6$  geometry, as shown in Figure 2.

**Electronic Spectra.** The electronic absorption spectra recorded in hexane and THF in the visible region are shown in Figure 3, and the CD spectrum recorded in THF is shown in Figure 4. The blue color clearly arises from the absorptions at  $\lambda_{\text{max}} \sim 580$  and 450 nm, which have  $\epsilon \sim 150$  and 100  $\text{dm}^3 \text{mol}^{-1} \text{cm}^{-1}$ , respectively. At shorter wavelengths, there is also a shoulder at  $\lambda \sim 380$  nm, and at ca. 300 nm, intense charge-transfer bands ( $\text{O}$  to  $\text{M}$ ) are observed.

The observation of a band at 580 nm is most unusual for  $d^3-d^3$  triply bonded complexes and certainly warrants attention. Complexes having the formula  $\text{M}_2\text{X}_6$  with ethane-like geometries are pale yellow or orange as the result of a tailing into the visible region of the spectrum of a band at ca. 300 nm arising from the  $\text{M}-\text{M} \pi$  to  $\text{M}-\text{M} (\pi/\delta)^*$  transition.<sup>14</sup> To interrogate

(9) Chisholm, M. H.; Cotton, F. A.; Murillo, C. A.; Reichert, W. W. *Inorg. Chem.* **1977**, *16*, 1801.

(10) Chisholm, M. H.; Cotton, F. A.; Frenz, B. A.; Reichert, W. W.; Shive, L. W.; Stults, B. R. *J. Am. Chem. Soc.* **1976**, *98*, 4469.

(11) Akiyama, M.; Chisholm, M. H.; Cotton, F. A.; Extine, M. W.; Haitko, D. A.; Little, D.; Fanwick, P. E. *Inorg. Chem.* **1979**, *18*, 2321.

(12) Chisholm, M. H.; Cotton, F. A.; Extine, M. W.; Stults, B. R. *J. Am. Chem. Soc.* **1976**, *98*, 4477.

(13) Cayton, R. H.; Chisholm, M. H. *Inorg. Chem.* **1991**, *30*, 1422 and references therein.

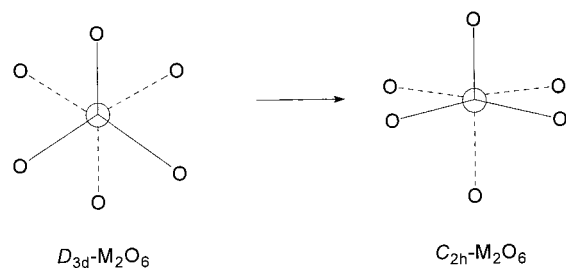


**Figure 2.** The  $D_{3d}$ - $\text{Mo}_2(\text{OH})_6$  to  $C_{2h}$ - $\text{Mo}_2(\text{OH})_6$  distortion shown as a Newman projection.

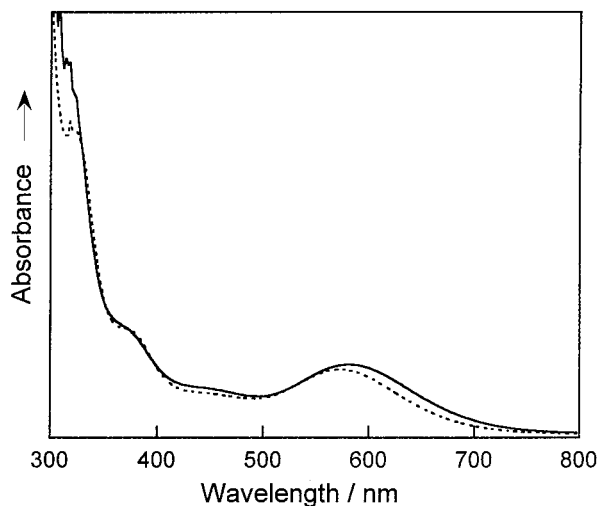


**Figure 3.** Visible absorption spectra of  $\text{Mo}_2\text{L}_2$  in hexane (solid line) and THF (dotted line).

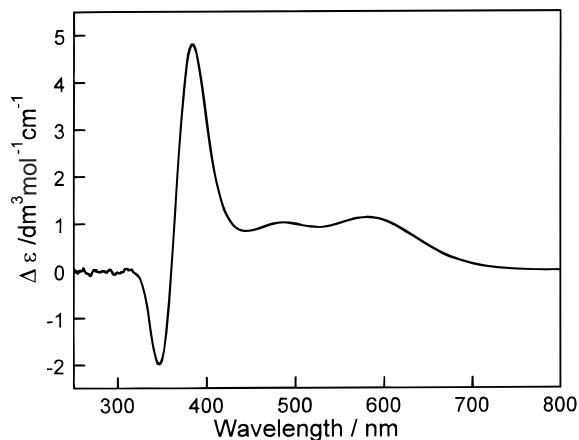


**Figure 4.** CD spectrum of  $\text{Mo}_2\text{L}_2$  in THF.

the electronic structure of  $\text{Mo}_2\text{L}_2$ , we undertook various molecular orbital calculations.

**Computed Structure.** By using the B3LYP DFT computational method, with the LANL2MB effective core potential and basis set, we examined the electronic structure of an idealized  $D_{3d}$ - $\text{Mo}_2(\text{OH})_6$  molecule with  $\text{Mo}-\text{Mo} = 2.19 \text{ \AA}$ ,  $\text{Mo}-\text{O} = 1.89 \text{ \AA}$ , and  $\text{Mo}-\text{Mo}-\text{O} = 103^\circ$ , which are typical structural features for a  $\text{Mo}_2(\text{OR})_6$  compound. The HOMO is a degenerate orbital of  $e_u$  symmetry having principally M-M  $d_\pi-d_\pi$  character. The LUMO is the M-M  $\delta^*$  orbital,  $e_g$ , which has some M-O  $\pi^*$  character. The SLUMO is of  $a_u$  symmetry and is principally M-M ( $d_{z^2}-d_{z^2}$ )  $\sigma^*$  in character, while the next highest orbital is the vacant degenerate M-M (p-p)  $\pi$  bonding

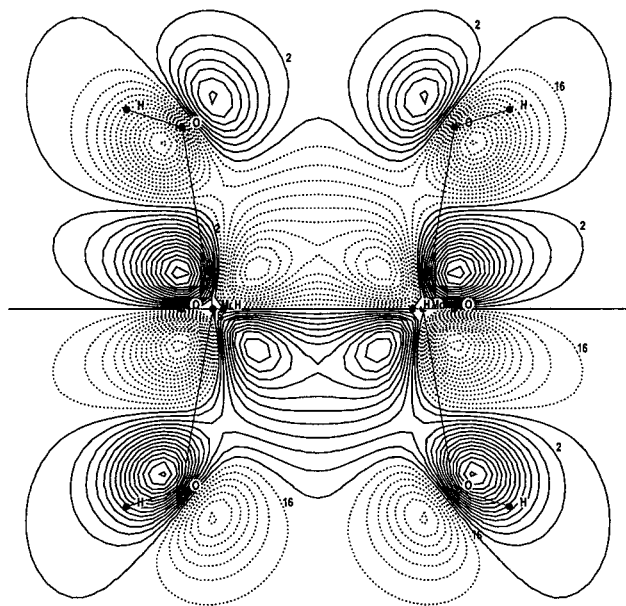


**Figure 5.** Contour plot of the HOMO drawn perpendicular to the  $\sigma_h$  plane.

orbital of  $e_u$  symmetry. These findings parallel other investigations of the electronic structure of  $\text{Mo}_2(\text{OR})_6$  molecules.<sup>2</sup>

To approximate the observed structure, calculations were performed on a molecule of the formula  $\text{Mo}_2(\text{OH})_6(\text{NH}_3)_2$  where the  $\text{Mo}_2\text{O}_6\text{N}_2$  skeleton was taken from the observed structure and the O-H bonds were substituted for O-C bonds. This low-symmetry molecule was subsequently sacrificed in favor of an idealized  $\text{Mo}_2(\text{OH})_6$  structure with  $C_{2h}$  symmetry. The removal of the  $\text{NH}_3$  ligands and the transformation to the idealized  $C_{2h}$  symmetry did not significantly change the orbital energies of the frontier MO's but did allow us to attempt to classify the MO's into  $\sigma$ ,  $\pi$ , and  $\delta$  components.

For a  $C_{2h}$ - $\text{Mo}_2(\text{OH})_6$  molecule, the M-M  $\pi$  orbitals are not degenerate and care must be taken to plot these orbitals in the appropriate plane. The HOMO is of  $a_u$  symmetry and the SHOMO of  $b_u$  symmetry. Both are M-M  $d_\pi-d_\pi$  bonding and M-O antibonding. They are shown in Figures 5 and 6, respectively, where it can be seen that the HOMO has a greater percentage of M-O  $\pi^*$  antibonding character. The calculated difference in energy between these orbitals is ca. 0.6 eV.

The LUMO is shown in Figure 7. It has  $a_g$  symmetry and is primarily M-M  $\pi^*$  in character. The SLUMO is of  $b_u$  symmetry and has primarily M-O  $\sigma^*$  character with metal s-p mixing. This is shown in Figure 8. The next highest orbital is shown in Figure 9 and has primarily oxygen lone pair character with some M-M ( $p_\pi-p_\pi$ )  $\pi^*$  contribution. In all of these orbitals, it is important to recognize how a classification such as M-M  $\sigma$ ,  $\pi$ , or  $\delta$  is compromised by the metal-oxygen admixture and by the lower symmetry of the complex.

These simple calculations show that the M-M frontier orbitals of the  $C_{2h}$ - $\text{Mo}_2(\text{OH})_6$  molecule are very different from those of the  $D_{3d}$ -(ethane-like) $\text{Mo}_2(\text{OH})_6$  molecule, where the orbitals all transform as "a" or "e".

The orbital energies deduced from the calculations are listed in Table 3 for the  $C_{2h}$ - $\text{Mo}_2(\text{OH})_6$  molecule. The HOMO-LUMO singlet transition is predicted to be the symmetry-allowed  $a_u$  to  $a_g$  orbital (a filled  $\pi$  to  $\pi^*$  type transition), and it is not unreasonable to assign this to the observed absorption at  $\lambda_{\text{max}} \sim 580 \text{ nm}$ , which causes this compound to be blue. The  $a_u$ (HOMO) to  $b_u$ (SLUMO) transition, which in  $C_{2h}$  symmetry is orbitally forbidden, may well correspond to the weaker band

(14) Chisholm, M. H.; Clark, D. L.; Kober, E. M.; Van Der Sluys, W. G. *Polyhedron* **1987**, *6*, 723.



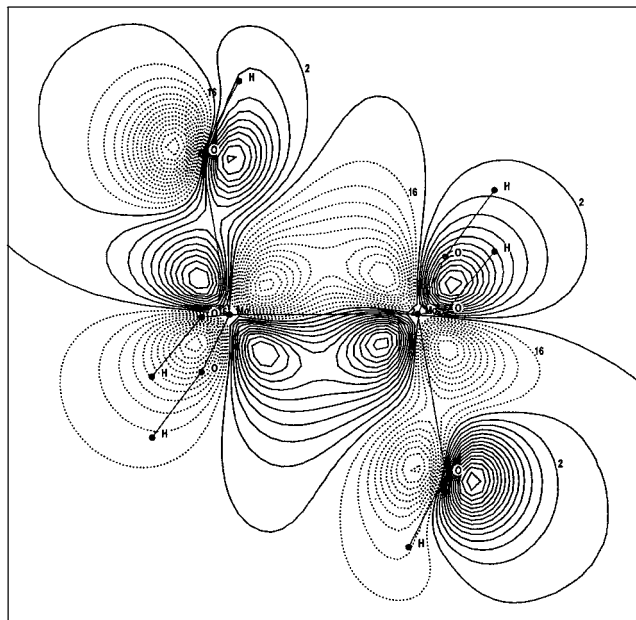


Figure 6. Contour plot of the SHOMO drawn in the  $\sigma_h$  plane.

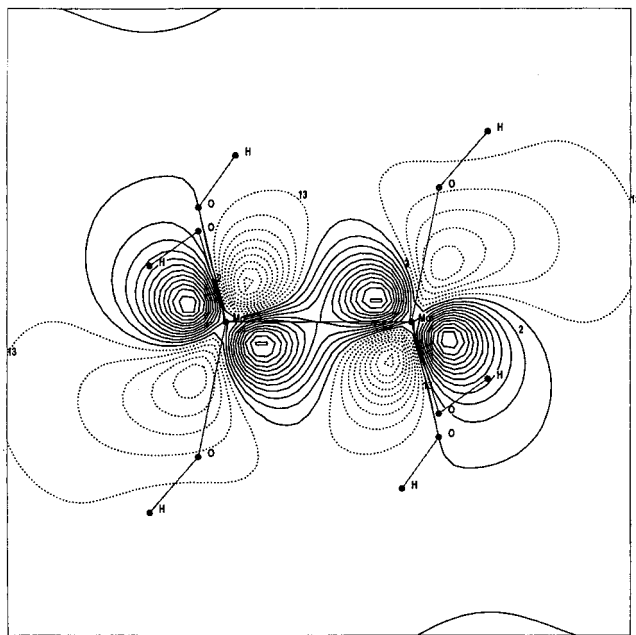


Figure 7. Contour plot of the LUMO drawn in the  $\sigma_h$  plane.

at  $\lambda_{\max} \sim 450$  nm; the  $a_u \rightarrow b_g$  (M–M  $p_\pi-p_\pi$ ,  $\pi^*$ ) transition is allowed and would be expected to have a much higher intensity, possessing significant metal  $d \rightarrow p$  character.

**Raman Spectra.** The assignment of  $\nu(\text{M–M})$  in the spectra of  $D_{3d}-\text{M}_2\text{X}_6$  compounds, where X = NMe<sub>2</sub> or OR (M = Mo or W), has proved problematic because of extensive coupling with metal–ligand vibrations.<sup>10,12</sup> However, for certain  $\text{M}_2(\text{OR})_6$  compounds, the assignment of  $\nu(\text{M}\equiv\text{M})$  has been proposed.<sup>15</sup> For the now classical quadruply bonded  $\text{M}_2\text{X}_8^{4-}$  complexes with  $D_{4h}$  symmetry, the assignment of  $\nu(\text{M–M})$  shows a similar complication as a function of X and the M–M–X angle.<sup>16–18</sup> In the present case, the  $\text{Mo}_2\text{O}_6\text{N}_2$  unit has approximately  $C_{2h}$

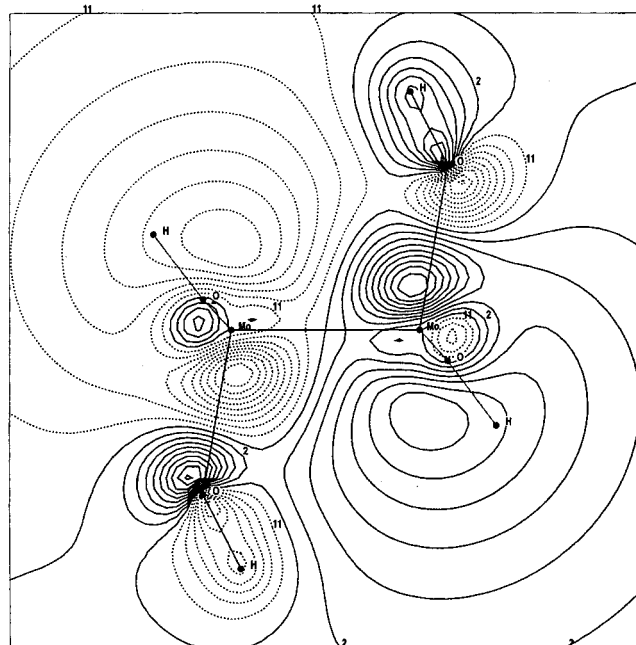


Figure 8. Contour plot of the SLUMO drawn in the  $\sigma_h$  plane.

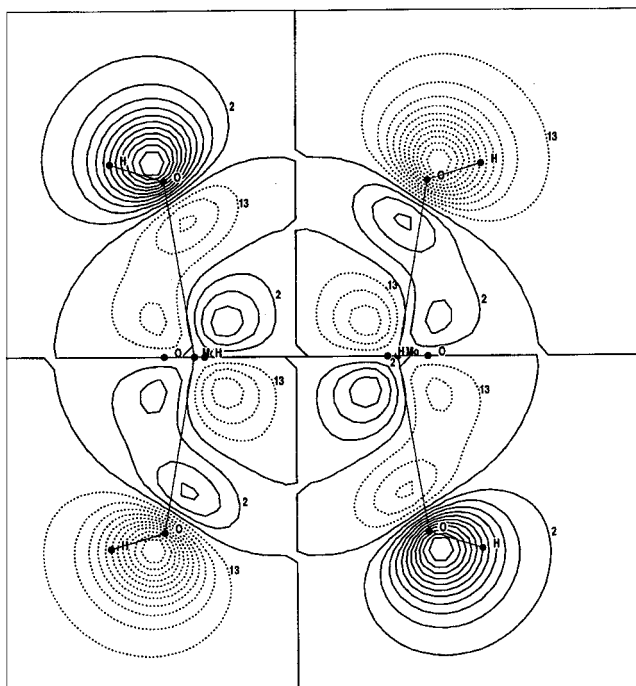


Figure 9. Contour plot of the vacant M–M ( $p_\pi-p_\pi$ )  $\pi^*$  molecular orbital.

Table 3. Orbital Energies (eV) of the Frontier MO's of a  $C_{2h}-\text{Mo}_2(\text{OH})_6$  Molecule as Deduced from the Calculations

SHOMO	−4.50	LUMO	−1.02
HOMO	−2.68	SLUMO	−0.96

symmetry, so the Mo–O stretches span  $2A_g + B_g + A_u + 2B_u$ , the MoN stretches span  $A_g + B_u$ , and the Mo–Mo stretch is designated as  $A_g$ . Five bands are therefore expected in the low-wavenumber region of the Raman spectrum. The  $\text{Mo}\equiv\text{Mo}$  triple-bond stretch is typically found near  $360\text{ cm}^{-1}$ .<sup>2</sup> For  $\text{Mo}_2(\text{O}_2\text{CCH}_3)_4$ , the Mo–O bond lengths (2.11–2.14 Å)<sup>19</sup> are

(15) Littrell, J. C.; Talley, C. E.; Dallinger, R. F.; Gilbert, T. M. *Inorg. Chem.* **1997**, *36*, 760.

(16) Clark, R. J. H.; Stead, M. J. *Inorg. Chem.* **1983**, *22*, 1214.

(17) Clark, R. J. H.; Hempleman, A. J.; Kurmoo, M. *J. Chem. Soc., Dalton Trans.* **1988**, 973.

(18) John, K. D.; Miskowski, V. M.; Vance, M. A.; Dallinger, R. F.; Wang, L. C.; Weib, S. J.; Hopkins, M. D. *Inorg. Chem.* **1998**, *37*, 6858 and references therein.

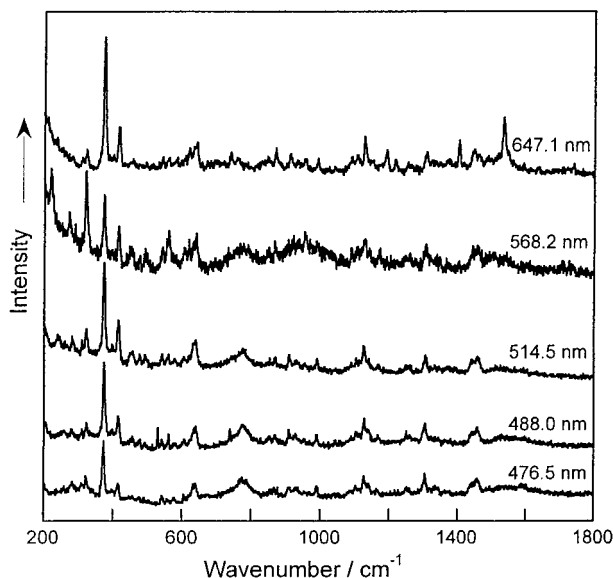


**Figure 10.** Raman spectra of  $\text{Mo}_2\text{L}_2$  at various excitation wavelengths.

longer than those for  $\text{Mo}_2\text{L}_2$  (1.86–2.02 Å), and so the  $\nu(\text{Mo}-\text{O})$  values for the former (301–323  $\text{cm}^{-1}$ )<sup>17</sup> would be expected to lie below those for the latter. The long Mo–N bond (ca. 2.4 Å) means that the Mo–N stretch should occur at even lower wavenumber, below 300  $\text{cm}^{-1}$ . It must be remembered, however, that four of the five Raman-active vibrational modes have the same symmetry and can mutually interact.

Samples of  $\text{Mo}_2\text{L}_2$  in the form of a mixture with KCl were examined as pressed disks at liquid-nitrogen temperature. Since the complex is blue, we obtained Raman spectra at various wavelengths, and this revealed some fascinating spectral changes. Raman spectra of  $\text{Mo}_2\text{L}_2$  recorded in KCl at excitation wavelengths ranging from 647.1 to 476.5 nm are shown in Figure 10. The spectra show a number of interesting features. First, five bands are seen between 280 and 414  $\text{cm}^{-1}$ . The spectrum recorded at 568.2 nm, near the peak of the electronic band, shows strong enhancement of the 322  $\text{cm}^{-1}$  band, lesser enhancement of the 373 and 414  $\text{cm}^{-1}$  bands, and the appearance of a strong band at 217  $\text{cm}^{-1}$ , possibly arising from a deformation mode. Raman band intensities were measured relative to that of the  $\nu_1(a_1)$  band of perchlorate in  $\text{KClO}_4$  as the internal standard; however, as this matrix for  $\text{Mo}_2\text{L}_2$  was less thermally stable than that formed in KCl, only qualitative excitation profiles could be obtained. These have been plotted in Figure 11, where it can be seen that there is an approximate correlation with the electronic band profile. The assignments of the Raman bands and the interpretations of the excitation profiles are complicated by both the mixing of the vibrational modes and the mixing of the Mo–Mo and Mo–O orbitals. A tentative assignment is that the highly enhanced 322  $\text{cm}^{-1}$  band has a high percentage of Mo–Mo character while the less enhanced 373 and 414  $\text{cm}^{-1}$  bands are best described as arising from  $A_g$  Mo–O stretches with some Mo–Mo character. The unenhanced 310 and 280  $\text{cm}^{-1}$  bands are then assigned to the  $B_g$  Mo–O stretch and the Mo–N stretch, respectively. These tentative assignments, along with a tabulation of the observed band maxima, are given in Table 4.

These spectra are notable for an extensive series of combination bands between 490 and 1500  $\text{cm}^{-1}$ . These are present even at the longest wavelength used, 647.1 nm, on the low-energy

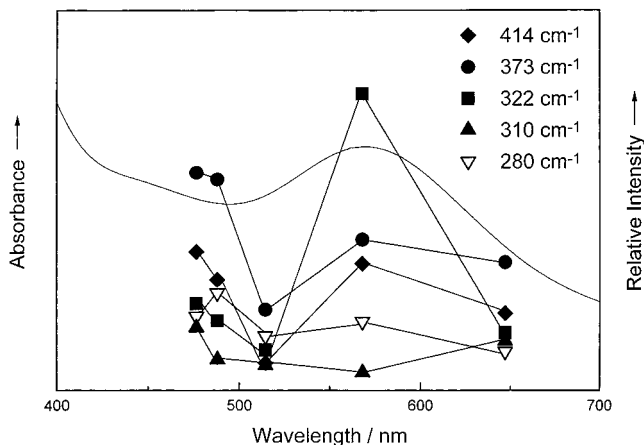


**Figure 11.** Excitation profiles of the Raman bands of  $\text{Mo}_2\text{L}_2$  at 414, 373, 322, 310, and 280  $\text{cm}^{-1}$ , together with the electronic spectrum.

edge of the HOMO–LUMO band centered at 580 nm. It is interesting to note that most of these combination bands involve the mode at 217  $\text{cm}^{-1}$  (probably a deformation mode) rather than the metal–metal stretch, as is often the case for multiply bonded metal–metal complexes. This implies that the geometric change on electronic excitation involves changes in both Mo–O(N) bond lengths and the Mo–Mo–O(N) angles (ca 99°), leading to a change of geometry around the ligand “cage”, with only a small change in the Mo–Mo bond length. This is consistent with the mixing of Mo–Mo and Mo–O orbitals indicated by the calculations.

### Concluding Remarks

The use of the (*S,S,S*)-triisopropanolamine to generate the dimolybdenum bis(triolate)  $\text{Mo}_2\text{L}_2$  has, by virtue of its coordination requirements, yielded an unusual  $d^3-d^3$  compound. Though the M–M bond is not directly bridged by oxygen atoms, the geometry of the  $\text{O}_6\text{N}_2$  unit imposes an unusual electronic configuration on the  $\text{Mo}_2^{6+}$  unit. The degeneracy of the  $e$  molecular orbitals ( $\pi$ ,  $\delta$ ,  $\pi^*$ ,  $\delta^*$ ) is removed, and extensive mixing of M–M and M–O bonding is evident from the calculations. Nevertheless, the  $d^3-d^3$  interaction can be said to give rise to a formal M–M triple bond of the type  $\sigma^2\pi_b^2\pi_a^2$ . The LUMO is clearly predicted by the calculations to have M–M  $\pi^*$  character, while the SLUMO has M–M  $\sigma^*$  character with considerable admixture of metal  $sp$  and oxygen character. The unusual blue color for an M–M triply bonded complex can reasonably be considered to arise from the low-energy singlet–singlet transition, HOMO  $\rightarrow$  LUMO, at 580 nm. The Raman spectra show complex but interesting resonance enhancements as the absorption band at 580 nm is traversed. The Raman band at 322  $\text{cm}^{-1}$  can reasonably be stated to have significant Mo–Mo character.

### Experimental Section

**General Procedures.** All syntheses and sample manipulations were carried out under an atmosphere of dry and deoxygenated nitrogen with standard Schlenk and glovebox techniques. Hydrocarbon solvents were distilled under  $\text{N}_2$  from Na/benzophenone and stored over 4 Å molecular sieves. Spectra were recorded on a Varian XL-300 (300 MHz) spectrometer in dry and deoxygenated benzene- $d_6$  or toluene- $d_8$ . All  $^1\text{H}$  and  $^{13}\text{C}$  NMR chemical shifts are reported in ppm relative to the residual protio impurities or  $^{13}\text{C}$  signals of the deuterated solvents. Infrared spectra were obtained from KBr pellets with a Nicolet S10P FT-IR spectrometer.

**Chemicals.** The preparations of  $\text{M}_2(\text{NMe}_2)_6$  (M = Mo, W) and  $\text{M}_2(\text{O}^i\text{Bu})_6$  (M = Mo, W) have been described previously.<sup>9–12</sup> The

(19) Cotton, F. A.; Mester, Z. C.; Webb, T. R. *Acta Crystallogr., Sect. B* 1974, 30, 2767.

**Table 4.** Wavenumbers and Tentative Assignments of Bands in the Raman Spectrum of Mo<sub>2</sub>L<sub>2</sub>

$\nu$ , cm <sup>-1</sup>	assignment	$\nu$ , cm <sup>-1</sup>	assignment
217 <sup>a</sup> s		1088 w	2 × 217 + 280 + 373 = 1087
247 vw, br		1103 w	
280 <sup>b</sup> vw	$\nu(\text{Mo-N})?$	1125 m	2 × 217 + 322 + 373 = 1129
310 w	$\nu(\text{Mo-O})$	1143 <sup>b</sup> w	
322 m <sup>c</sup>	$\nu(\text{Mo-Mo})$	1167 vw	2 × 217 + 322 + 414 = 1170
373 s	$\nu(\text{Mo-O})$	1188 m	
414 m	$\nu(\text{Mo-O})$	1214 m	2 × 217 + 776 = 1210
454 w		1253 w	
476 w		1305 m	CH <sub>2</sub> wag
493 w	217 + 280 = 497	1318 w	
542 w	217 + 322 = 539	1336 vw	
559 w		1386 vw	3 × 217 + 322 + 414 = 1387
577 vw		1398 m	CH def
635 m	217 + 414 = 631 and/or 310 + 322 = 632	1442 w	217 + 454 + 776 = 1447
		1459 <sup>b</sup> w	217 + 476 + 776 = 1469
684 m	310 + 373 = 683	1530 m	CH <sub>3</sub> def
737 w	322 + 414 = 736	1590 vw	
758 vw		2518 vw	
776 <sup>b</sup> m, br		2847 w	$\nu(\text{C-H})$
846 w	2 × 217 + 414 = 848	2878 w	$\nu(\text{C-H})$
868 m	217 + 280 + 373 = 870	2891 w	$\nu(\text{C-H})$
910 w	217 + 322 + 373 = 912	2928 m	$\nu(\text{C-H})$
929 vw		2966 m	$\nu(\text{C-H})$
954 w	217 + 322 + 414 = 953	3042 m	$\nu(\text{C-H})$
990 w	217 + 776 = 993		

<sup>a</sup> The intensity designations s, m, w, and vs pertain to 647.1 nm excitation and may be substantially different with other excitations. In particular, the band at 217 cm<sup>-1</sup> is only seen with 568.2 nm excitation. <sup>b</sup> Bands appearing at 280, 776, 1143 and 1459 cm<sup>-1</sup> occur 4–7 cm<sup>-1</sup> lower with 568.2 nm excitation than with 476.5, 488.0, 514.5, and 647.1 nm excitation. The reason for this is not clear. <sup>c</sup> This band is the most intense in the whole spectrum with 568.2 nm excitation.

ligand (S,S,S)-triisopropanolamine was synthesized from (S)-propylene oxide and (S)-1-amino-2-propanol (Aldrich).<sup>8</sup>

**Mo<sub>2</sub>L<sub>2</sub> (L = N(CH<sub>2</sub>CHMeO<sup>-</sup>)<sub>3</sub>).** A reaction mixture of Mo<sub>2</sub>(OBU)<sub>6</sub> (315 mg, 0.50 mmol) and (S,S,S)-triisopropanolamine (195 mg, 1.0 mmol) in 20 dm<sup>3</sup> of benzene was stirred at room temperature for 2 h to obtain a blue solution. The volatile components were removed in vacuo, and the residue was suspended in hexane to give a blue precipitate, Mo<sub>2</sub>L<sub>2</sub>, which was collected and dried in vacuo (241 mg, yield 83%). The compound Mo<sub>2</sub>L<sub>2</sub> could also be synthesized from a reaction mixture of Mo<sub>2</sub>(NMe<sub>2</sub>)<sub>6</sub> and (S,S,S)-triisopropanolamine in a similar yield. Crystals of Mo<sub>2</sub>L<sub>2</sub>·2C<sub>6</sub>H<sub>6</sub> suitable for X-ray analysis were obtained by slow evaporation of a benzene solution. Anal. Calcd (found) for C<sub>30</sub>H<sub>48</sub>O<sub>6</sub>N<sub>2</sub>Mo<sub>2</sub>: C, 49.73 (49.65); H, 6.68 (6.60); N, 3.87 (3.96). <sup>1</sup>H NMR (300 MHz, 20 °C, benzene-*d*<sub>6</sub>): CH,  $\delta$  5.42 (m, 2H),  $\delta$  5.27 (m, 2H),  $\delta$  3.51 (m, 2H); CH<sub>2</sub>,  $\delta$  2.85 (m, 2H),  $\delta$  2.56 (m, 2H),  $\delta$  2.07 (m, 2H),  $\delta$  1.78 (m, 2H),  $\delta$  1.67 (m, 2H),  $\delta$  1.44 (m, 2H); CH<sub>3</sub>,  $\delta$  1.36 (d, 6H),  $\delta$  1.29 (d, 6H),  $\delta$  1.18 (d, 6H). <sup>13</sup>C{<sup>1</sup>H} NMR (125 MHz, 20 °C, benzene-*d*<sub>6</sub>): CH,  $\delta$  75.11,  $\delta$  73.86,  $\delta$  70.52; CH<sub>2</sub>,  $\delta$  69.25,  $\delta$  68.38,  $\delta$  65.12; CH<sub>3</sub>,  $\delta$  22.82,  $\delta$  23.42,  $\delta$  21.47.

**W<sub>2</sub>L<sub>2</sub> (L = N(CH<sub>2</sub>CHMeO<sup>-</sup>)<sub>3</sub>).** A reaction mixture of W<sub>2</sub>(OBU)<sub>6</sub> (402 mg, 0.50 mmol) and (S,S,S)-triisopropanolamine (192 mg, 1.0 mmol) in 15 dm<sup>3</sup> of benzene was stirred at room temperature for 4 h to obtain a blue solution. The volatile components were removed in vacuo, and the residue was washed with hexane to give a green powder, W<sub>2</sub>L<sub>2</sub>, which was dried in vacuo (213 mg, yield 67%). The compound W<sub>2</sub>L<sub>2</sub> could also be synthesized from a reaction mixture of W<sub>2</sub>(NMe<sub>2</sub>)<sub>6</sub> and (S,S,S)-triisopropanolamine in a similar yield. <sup>1</sup>H NMR (300 MHz, 20 °C, benzene-*d*<sub>6</sub>): CH,  $\delta$  5.54 (m, 2H),  $\delta$  5.33 (m, 2H),  $\delta$  3.43 (m, 2H); CH<sub>2</sub>,  $\delta$  2.96 (m, 2H),  $\delta$  2.31 (m, 2H),  $\delta$  2.19 (m, 2H),  $\delta$  1.79 (m, 2H),  $\delta$  1.60 (m, 2H),  $\delta$  1.44 (m, 2H); CH<sub>3</sub>,  $\delta$  1.39 (d, 2H),  $\delta$  1.24 (d, 6H),  $\delta$  1.17 (d, 6H). <sup>13</sup>C{<sup>1</sup>H} NMR (125 MHz, 20 °C, benzene-*d*<sub>6</sub>): CH,  $\delta$  76.88,  $\delta$  72.49,  $\delta$  72.27; CH<sub>2</sub>,  $\delta$  69.48,  $\delta$  68.51,  $\delta$  66.25; CH<sub>3</sub>,  $\delta$  23.81,  $\delta$  23.32,  $\delta$  21.14.

**Crystallographic Studies.** General operating procedures and a list of programs have been given previously,<sup>20</sup> and a summary of the crystal data is given in Table 5. Bright blue crystals were formed on the sides of the flask in the crystallizing medium. Several different crystals were

**Table 5.** Summary of Crystal Data

empirical formula	C <sub>30</sub> H <sub>48</sub> Mo <sub>2</sub> N <sub>2</sub> O <sub>6</sub>
color of crystal	blue
crystal system; space group	monoclinic: C2
<i>a</i> , Å	17.389(6)
<i>b</i> , Å	10.843(3)
<i>c</i> , Å	10.463(3)
$\alpha$ , deg	90.00(0)
$\beta$ , deg	125.28(1)
$\gamma$ , deg	90.00(0)
<i>V</i> , Å <sup>3</sup>	1610.45
<i>Z</i> , molecules/cell	2
<i>d</i> <sub>calcd</sub> , g dm <sup>-3</sup>	1.494
<i>M<sub>r</sub></i>	724.60
linear abs coeff, cm <sup>-1</sup>	8.195
<i>R</i> ( <i>F</i> ) <sup>a</sup>	0.051
<i>R<sub>w</sub></i> ( <i>F</i> ) <sup>b</sup>	0.048

$$^a R(F) = \sum(|F_o| - |F_c|)/\sum|F_o|. \quad ^b R_w(F) = [\sum w(|F_o| - |F_c|)^2/\sum wF_o^2]^{1/2}.$$

$$R_w(F) = [\sum w(|F_o| - |F_c|)^2/(N_{\text{observns}} - N_{\text{variables}})]^{1/2}.$$

examined before a suitable sample was obtained because the crystals tended to lose solvent fairly rapidly. A systematic search of a limited hemisphere of reciprocal space was used to determine that the crystal possessed monoclinic symmetry with systematic absences corresponding to a C-centered cell but no other extinctions. Subsequent solution and refinement of the structure confirmed the noncentrosymmetric space group C2 as the proper choice. The data were collected using a standard moving crystal–moving detector technique with fixed backgrounds at each extreme of the scan. The data were then corrected for Lorentz and polarization effects, and equivalent reflections were averaged.

The structure was finally solved using direct methods (SHELX) and Fourier techniques. Because of the disorder present, some difficulty was encountered during the solution of the structure. While two Mo atom occupancies (Mo(1), 48% occupancy; Mo(2), 45% occupancy) dominate, the third (Mo(3), 6% occupancy) was initially thought to involve a disordered part of the ligand. When the nature of the disorder was finally resolved, the structure slowly converged. As shown for the thermal ellipsoids, there is probably a slight disorder in the ligands. All hydrogen atoms were placed in fixed idealized positions for the final cycles of the refinement. The structure can be described as

(20) Chisholm, M. H.; Folting, K.; Huffman, J. C.; Kirkpatrick, C. C. *Inorg. Chem.* **1984**, 23, 1021.

possess a pseudocubic coordination environment consisting of two nitrogen and six oxygen atoms, with the disordered Mo atoms in each face of the cube, and the six O atoms forming an octahedron. The molecule lies on the 2-fold axis of the cell, and a benzene solvent molecule is present as well.

The absolute structure was determined by examination of the residuals for the two enantiomers. A final difference Fourier map was featureless, with a maximum peak intensity of  $0.79 \text{ e}/\text{\AA}^3$ .

**Raman Spectra.** Raman spectra were recorded for the sample pressed into an approximately 50:50 disk with KCl and held in a purpose-built cryostat cooled with liquid nitrogen. Spectra were excited at wavelengths between 476.5 and 647.1 nm with radiation from Coherent Innova 70 Ar<sup>+</sup> and 301 Kr<sup>+</sup> lasers. The power at the sample ranged from 50 to 110 mW, depending on the laser line. The entrance slits of the Spex 1401 monochromator were set to give a spectral bandwidth of  $4 \text{ cm}^{-1}$  for each excitation wavelength. Band wavenumbers were calibrated by superimposing neon emission lines on the Raman spectra to give an estimated accuracy of  $\pm 1 \text{ cm}^{-1}$ .

The excitation profile was recorded at the wavelengths used for Raman excitation using a disk consisting of Mo<sub>2</sub>L<sub>2</sub>, KClO<sub>4</sub>, and KCl in the approximate proportion 2:1:1. Due to problems of sample burning and increased Rayleigh scattering, it was only possible to record excitation profiles of the 414 and 373  $\text{cm}^{-1}$  bands with this disk. Excitation profiles of the other bands were calculated from the relative intensities of the 373 and 414  $\text{cm}^{-1}$  bands in the appropriate KCl spectra. All spectra were corrected for the wavelength dependence of the spectrometer response.

**Computational Procedures.** The Mo–Mo and Mo–O distances and Mo–Mo–O angles used in the initial calculations were 2.19 and 1.89 Å and 103°, respectively, which are typical for Mo<sub>2</sub>(OR)<sub>6</sub> compounds.<sup>21</sup> Calculations on Mo<sub>2</sub>(OH)<sub>6</sub>(NH<sub>3</sub>)<sub>2</sub> were modeled on the

observed structural parameters observed for the Mo<sub>2</sub>L<sub>2</sub> complex reported here, where O–H was substituted for O–C and NH<sub>3</sub> was substituted for N(CH<sub>2</sub>)<sub>3</sub>. The data presented in this work pertaining to the idealized C<sub>2h</sub>-Mo<sub>2</sub>(OH)<sub>6</sub> molecule differed only qualitatively from those obtained for Mo<sub>2</sub>(OH)<sub>6</sub>(NH<sub>3</sub>)<sub>2</sub> and allowed a ready comparison with those found for the idealized D<sub>3d</sub>-Mo<sub>2</sub>(OH)<sub>6</sub> molecule. The B3LYP DFT calculations employed Gaussian 98.<sup>22</sup>

**Acknowledgment.** We thank the National Science Foundation for support of this work at Indiana University. R.J.H.C. and S.F. thank the University of London Intercollegiate Research Service for support.

**Supporting Information Available:** An X-ray crystallographic file, in CIF format, for the Mo<sub>2</sub>L<sub>2</sub> complex. This material is available free of charge via the Internet at <http://pubs.acs.org>.

IC991352D

- 
- (21) Chisholm, M. H. *Polyhedron* **1983**, *2*, 681.
- (22) Frisch, M. J.; Trucks, G. W.; Schlegel, H. B.; Scuseria, G. E.; Robb, M. A.; Cheeseman, J. R.; Zakrzewski, V. G.; Montgomery, J. A., Jr.; Stratmann, R. E.; Burant, J. C.; Dapprich, S.; Millam, J. M.; Daniels, A. D.; Kudin, K. N.; Strain, M. C.; Farkas, O.; Tomasi, J.; Barone, V.; Cossi, M.; Cammi, R.; Mennucci, B.; Pomelli, C.; Adamo, C.; Clifford, S.; Ochterski, J.; Petersson, G. A.; Ayala, P. Y.; Cui, Q.; Morokuma, K.; Malick, D. K.; Rabuck, A. D.; Raghavachari, K.; Foresman, J. B.; Cioslowski, J.; Ortiz, J. V.; Stefanov, B. B.; Liu, G.; Liashenko, A.; Piskorz, P.; Komaromi, I.; Gomperts, R.; Martin, R. L.; Fox, D. J.; Keith, T.; Al-Laham, M. A.; Peng, C. Y.; Nanayakkara, A.; Gonzalez, C.; Challacombe, M.; Gill, P. M. W.; Johnson, B.; Chen, W.; Wong, M. W.; Andres, J. L.; Gonzalez, C.; Head-Gordon, M.; Replogle, E. S.; Pople, J. A. *Gaussian 98*, Revision A.6; Gaussian, Inc.: Pittsburgh, PA, 1998.